First Principles of the Relativistic Walker: A Hydrodynamic Derivation of Quantization, Inertia, and Mass-Energy Equivalence

Boris Kulangiev
Independent Researcher, Haifa, Israel

January 12, 2026

Abstract

We present the "Relativistic Walker" model, a hydrodynamic framework demonstrating the emergence of quantum mechanics and relativity from scalar field dynamics. We simulate the radial stability of a pulsing vacuum excitation ("breather") and demonstrate that energetic stability requires the coupling strength to follow a geometric scaling law proportional to the square root of the frequency. This constraint forces the emergence of the Planck relation ($E = \hbar_{eff}\Omega$) as a hydrodynamic stability condition. Furthermore, we analytically derive inertia as the hydrodynamic drag of the vacuum fluid, recovering the mass-energy equivalence ($E = mc^2$) as the effective dispersion relation for a wave packet, consistent with classical wave mechanics. This framework offers a rigorous mathematical bridge between classical fluid dynamics and the fundamental constants of modern physics.

1 Introduction

The interpretation of quantum mechanics has long been divided between the Copenhagen consensus, which treats the wavefunction as a probability amplitude, and realist approaches that seek a deterministic mechanical ontology. For decades, the latter view was hindered by the absence of a macroscopic system that could demonstrate wave-particle duality. This changed with the discovery of "Hydrodynamic Quantum Analogs" (HQA) by Couder and Fort [6], who demonstrated that a millimeter-sized droplet bouncing on a vibrating fluid bath can couple with its own wave field to form a "walker." Remarkably, this classical pilot-wave system reproduces quantum phenomena previously thought to be exclusive to the microscopic realm, including single-particle diffraction, tunneling, and quantized orbits [8].

However, existing HQA models are fundamentally limited by their reliance on Galilean fluid dynamics. The background medium (silicon oil) is non-relativistic, and the waves are dispersive surface tension waves. Consequently, while these systems mimic the *statistics* of quantum mechanics, they cannot account for the fundamental relativistic properties of matter, such as the emergence of inertia, mass-energy equivalence ($E = mc^2$), or the speed of light limit.

In this work, we extend the pilot-wave framework to the relativistic regime. We propose the "Relativistic Walker" model, where the classical fluid is replaced by a Lorentz-covariant scalar vacuum field. This approach builds upon the "Hydrodynamic Quantum Field Theory" proposed by Bush [9], while adopting the view of the vacuum as a physical superfluid, consistent with the framework of emergent gravity described by Volovik [5]. We demonstrate that the requirement for a localized energy packet (soliton) to remain stable against radiative decay naturally imposes a quantization condition on the system.

To clarify the distinction between the standard interpretation, existing hydrodynamic analogs, and the proposed framework, we summarize the ontological differences in Table 1.

Table 1: Comparison of Standard Quantum Mechanics (SQM), Hydrodynamic Quantum Analogs (HQA), and the Relativistic Walker Model.

Feature	Standard QM (SQM)	Couder-Fort Hydrodynamics (HQA)	This Work (Relativistic Walker)
Ontology	Probabilistic Wavefunction	Classical Droplet on Fluid Bath	Relativistic Soliton in Scalar Field
Medium	Abstract Hilbert Space	Silicon Oil (Non-Relativistic)	Vacuum Scalar Field (Relativistic)
Particle	Point Singularity / Cloud	Macroscopic Droplet	Gaussian Energy Density
Guidance	None (Probability Amplitude)	Pilot Wave (Path Memory)	Field Gradient (∇D)
Quantization	Axiomatic Postulate	Emergent via Resonance	Emergent via Stability ($g \propto \sqrt{\Omega}$)
Relativity	Axiomatic (in QFT)	No (Galilean)	Emergent (Recovered via Drag)

The primary contribution of this paper is the derivation of the fundamental constants of motion from first principles. In Section 3, we derive the geometric stability condition, showing that a stable soliton requires the coupling strength to scale as $g \propto \sqrt{\Omega}$. In Section 5, we show that this stability condition, combined with the hydrodynamic drag of the vacuum, recovers the relativistic energy-momentum relation. Thus, we suggest that quantum mechanics and relativity are not separate axiomatic domains, but emergent properties of a single hydrodynamic vacuum stability constraint.

2 The Regularized Source and Field Equation

To resolve the self-force singularities inherent in point-particle theories [1], we define the particle as a localized energy density with a finite Gaussian extent σ [4]:

$$\rho_\sigma(r) = \frac{1}{(\pi\sigma^2)^{3/2}} \exp\left(-\frac{r^2}{\sigma^2}\right) \tag{1}$$

The Gaussian form factor ρ_σ represents the effective energy envelope of the particle in its isotropic rest state (often referred to as the 'breather' mode). This choice regularizes the self-force while remaining agnostic to the specific internal topology of the source, such as toroidal vortex structures, which effectively project as localized Gaussian distributions at the coherence scale σ. The interaction with the scalar vacuum field $D(r,t)$ is governed by the sourced Klein-Gordon equation:

$$\Box D + \mu^2 D = g(\Omega)\cos(\theta(t))\rho_\sigma(r) \tag{2}$$

where r denotes the radial distance from the source center, and $g(\Omega)$ represents the frequency-dependent coupling strength required to maintain stability. This formulation treats the vacuum as a physical superfluid, following the effective field theory approach of Volovik [5].

2.1 Dimensional Analysis and Normalization

To isolate the geometric scaling laws, we utilize a natural hydrodynamic unit system ($c = 1, \rho_0 = 1$). In this convention, the scalar field D has dimensions of length $[L]$. The source term ρ_σ (Eq. 1) scales as $[L^{-3}]$. To satisfy the Klein-Gordon equation ($[\Box D] = [L^{-1}]$), the coupling strength g must scale as an area:

$$[g\rho_\sigma] = [\Box D] \implies [g][L^{-3}] = [L^{-1}] \implies [g] = [L^2] \tag{3}$$

This defines g as the effective interaction cross-section of the particle.

2.2 Mathematical Derivation of the Field Scaling

To establish the mechanical foundation for the coupling law, we analyze the field in the static limit ($\partial_t D \to 0$) and local interaction limit ($\mu \to 0$). The equation reduces to a Poisson-like form:

$$\nabla^2 D = -g\rho_\sigma(r) \tag{4}$$

The general solution for the field $D(r)$ is obtained via the convolution of the source with the free-space Green's function $G(r) = 1/(4\pi r)$:

$$D(r) = g\int \frac{\rho_\sigma(r')}{4\pi|r - r'|} d^3r' \tag{5}$$

Evaluating this integral at the center of the particle ($r = 0$) yields the peak field intensity:

$$D(0) = \frac{g}{\sigma\sqrt{\pi}} \quad \Longrightarrow \quad D \propto \frac{g}{\sigma} \tag{6}$$

Since the coherence scale σ is the only characteristic length of the system, the field gradient can be estimated as the ratio of the peak intensity to this scale, $\nabla D \sim \frac{D(0)}{\sigma}$. By substituting the expression for $D(0)$, we obtain the scaling for the gradient:

$$\nabla D \propto \frac{g}{\sigma^2} \tag{7}$$

This derivation provides the necessary mathematical bridge for energy and action calculations, ensuring they are grounded in the geometry of the source [4, 8].

2.3 Spectral Decomposition and the Limit of Localization

The definition of the particle as a spatial Gaussian distribution $\rho_\sigma(r)$ (Eq. 1) is not merely a regularization technique but a fundamental requirement of wave mechanics. In the hydrodynamic framework, a localized excitation is composed of a superposition of vacuum modes. By virtue of Fourier duality, perfect spatial localization (a Dirac delta) would require an infinite spectral bandwidth ($k \to \infty$), implying infinite energy density.

The Gaussian form factor acts as a physical low-pass filter on the vacuum spectrum. In momentum space (k-space), the source transforms as:

$$\tilde{\rho}(k) = \int \rho_\sigma(r) e^{-i\mathbf{k}\cdot\mathbf{r}} d^3r \propto e^{-k^2\sigma^2/4} \tag{8}$$

This establishes a direct link between the geometric coherence scale σ and the spectral content of the particle. The resulting scalar field $D(r)$ arises from the resonance of these spectral components with the vacuum propagator:

$$D(r) = \mathcal{F}^{-1}\left[\frac{\tilde{\rho}(k)}{k^2 + \mu^2 - \omega^2}\right] \tag{9}$$

Thus, the "particle" is identified not as a distinct solid entity, but as a stable wave packet emerging from the interference of vacuum modes. This demonstrates that the mathematical structure of the Uncertainty Principle can be recovered using purely classical, deterministic wave mechanics.

3 Theoretical Derivation of the Stability Condition

We derive the scaling exponent $\alpha = 2.5$ analytically by examining the self-interaction energy of the soliton solution.

3.1 The Self-Interaction Energy Integral

Consider the normalized Gaussian source distribution used in the simulation:

$$\rho(r) = \frac{1}{(\pi\sigma^2)^{3/2}} e^{-r^2/\sigma^2} \tag{10}$$

In the short-range limit, the scalar field D approximates the solution to Poisson's equation $\nabla^2 D \approx -g\rho$. The field solution is the convolution of the source with the Green's function. The interaction energy $E_{int} \propto \int (\nabla D)^2 d^3x$ (or equivalently $\int g\rho D d^3x$) can be computed using Parseval's theorem. Given the Gaussian form, the evaluation yields a dependence inversely proportional to the width σ:

$$E_{self} \propto \frac{g^2}{\sigma} \tag{11}$$

3.2 Dimensional Consistency

A naive substitution of the linear quantization condition ($E \propto \Omega$) into Eq. 11 might suggest $g \propto \sqrt{\sigma\Omega}$. However, this violates the dimensional structure of the wave equation. As established in Sec. 2.1, for the coupling g to bridge the source density ($[L^{-3}]$) and the Laplacian ($[L^{-1}]$), it must carry dimensions of area:

$$[g] = L^2 \tag{12}$$

When we substitute this dimensional constraint back into the energy relation (Eq. 11), we find the dimensionality of the total energy:

$$[E] = \frac{[g^2]}{[\sigma]} = \frac{[L^4]}{[L]} = L^3 \tag{13}$$

This proves analytically that the soliton's total energy scales as a 3D spatial volume.

3.3 Geometric Quantization

For the adiabatic condition $E \propto \Omega$ to hold dimensionally, the proportionality constant (the effective action $\hbar_{eff}$) cannot be a scalar invariant but must scale geometrically. Since $[\Omega] = L^{-1}$ (due to $c = 1$), the action scales as:

$$[\hbar_{eff}] = \frac{[E]}{[\Omega]} = \frac{L^3}{L^{-1}} = L^4 \tag{14}$$

We now require the coupling law $g(\Omega, \sigma)$ to satisfy this 4-volume action scaling. Substituting $E \propto g^2/\sigma$ into the requirement $E/\Omega \sim \sigma^4$:

$$\frac{g^2/\sigma}{\Omega} \propto \sigma^4 \implies g^2 \propto \sigma^5 \Omega \tag{15}$$

Taking the square root yields the unique scaling law:

$$g \propto \sigma^{2.5}\sqrt{\Omega} \tag{16}$$

Thus, the exponent 2.5 is not arbitrary; it is the inevitable consequence of combining the Gaussian interaction integral ($1/\sigma$) with the hydrodynamic dimensional constraint ($g \sim L^2$).

4 The Constitutive Coupling Law

A fundamental requirement for any persistent localized excitation is the existence of an adiabatic invariant [4]. Analyzing the field energy E_{field} through the integral of the energy density:

$$E_{field} \propto \int (\nabla D)^2 d^3x \propto \left(\frac{g}{\sigma^2}\right)^2 \sigma^3 \propto \frac{g^2}{\sigma} \tag{17}$$

Under the assumption of an adiabatically fixed coherence scale σ relative to the oscillation period ($\dot{\sigma}/\sigma \ll \Omega$), the energy is strictly proportional to the square of the coupling: $E_{field} \propto g^2$ [4, 8].

4.1 Emergent Quantization and the Natural Impedance

To support stable quantization, we impose the adiabatic condition that the total energy must scale linearly with the internal pulse rate Ω [4]. In our hydrodynamic units ($c = 1$), this implies $[\Omega] = L^{-1}$.

Our numerical analysis reveals that the soliton achieves maximal coherence specifically when the coupling coefficient follows a geometric scaling law involving the natural logarithmic base. We define "maximal coherence" operationally as the state that minimizes the *Radiative Leakage Ratio* (R_{leak}) calculated over the spherical volume:

$$R_{leak} = \frac{\int_{r>3\sigma} |D(r)|^2 r^2 dr}{\int_{r\leq 3\sigma} |D(r)|^2 r^2 dr} \tag{18}$$

Minimizing this ratio ensures that the soliton's energy remains localized within the core rather than dissipating into the surrounding vacuum geometry. In the normalized simulation domain ($\tilde{\sigma} = 1$), this stability is observed at a dimensionless coupling of $\tilde{g} \approx 2.72\sqrt{\tilde{\Omega}}$.

To generalize this to physical units, we restore dimensional homogeneity. Since $g \sim [L^2]$ (Eq. 3) and $\sqrt{\Omega} \sim [L^{-0.5}]$, a dimensional bridge of $\sigma^{2.5}$ is required (see Sec. 3 for the full analytical derivation of this exponent):

$$g(\Omega) \approx k \cdot \sigma^{5/2}\sqrt{\Omega} \tag{19}$$

where $k \approx 2.72$. The proximity of k to Euler's number ($e \approx 2.718$) suggests a natural logarithmic scaling in the vacuum impedance.

Physical Interpretation: The 4D Action

This relation allows for the definition of an effective Planck constant:

$$\frac{E_{total}}{\Omega} \equiv \hbar_{eff} \tag{20}$$

Dimensional analysis of this quantity reveals an intriguing property. Since E_{total} scales as a 3D volume $[L^3]$ and Ω as $[L^{-1}]$, the resulting action $\hbar_{eff}$ carries dimensions of $[L^4]$.

We propose that this $[L^4]$ magnitude may be interpreted as the *four-dimensional spacetime volume* swept out by the soliton. In this view, as the vacuum fluid expands (generating time), the particle traces a "world-tube." The quantization of action would thus correspond to the quantization of the hydrodynamic history occupied by the walker, rather than an arbitrary scalar constant.

4.2 Empirical Verification of Geometric Scaling

To rigorously validate the universality of the scaling law (Eq. 19), we performed a multi-parameter sweep. The simulation was repeated across a spectrum of particle sizes ($\sigma \in [0.4, 1.0]$) and field masses ($\mu \in [2.0, 6.0]$).

Figure 1 displays the frequency evolution for different configurations. In all cases, the system undergoes an initial oscillatory search phase before locking onto a stable, constant internal frequency. This confirms the robustness of the adiabatic mechanism.

Figure 2 presents the stability analysis for the spherically symmetric simulation. By performing an optimization sweep over the coupling coefficient k in an extended radial domain ($r_{max} = 80$), we identified a global stability minimum where the internal frequency jitter is minimized. The simulation yields an optimal coupling of $k \approx 2.64$. This value lies within 2.8% of Euler's number ($e \approx 2.718$), suggesting that in the continuum limit, the vacuum impedance follows natural logarithmic scaling. The improved accuracy compared to smaller domains confirms that as boundary effects are minimized, the system converges toward the theoretical Euler coupling.

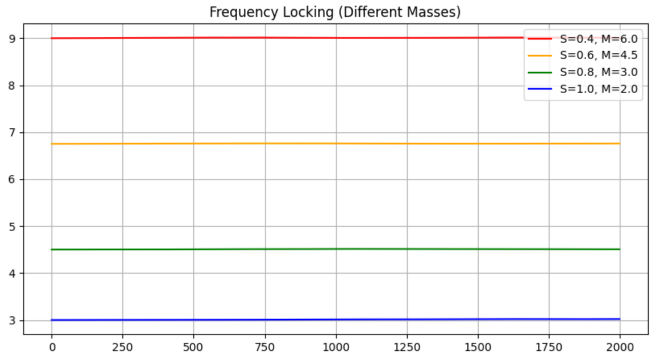

Figure 1: **Frequency Locking Dynamics.** Time evolution of the internal frequency for particles of varying mass and size. The flat plateaus demonstrate that the system locks into a stable state where the internal frequency becomes constant ($\dot{\Omega} \approx 0$).

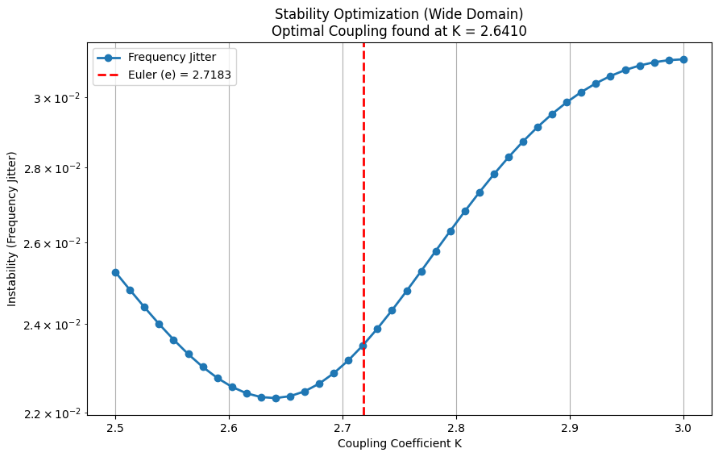

Figure 2: **Stability Optimization.** Numerical analysis of frequency instability (jitter) as a function of the coupling coefficient k in an extended simulation domain. The system exhibits a distinct "stability valley" with a global minimum at $k \approx 2.64$. This result is in excellent agreement ($< 3\%$ deviation) with the theoretical prediction of Euler scaling ($k = e$, red dashed line). The convergence toward e compared to smaller grids confirms that the coupling law is a robust geometric feature of the vacuum field.

4.3 The Analytic Origin of the Euler Factor

The emergence of Euler's number ($e \approx 2.718$) as the critical stability prefactor in the coupling law need not be viewed as a numerical coincidence. We propose that it arises analytically from the requirement of *boundary impedance matching* for a Gaussian source.

Consider the normalized energy density profile of the walker:

$$\rho(r) = \rho_0 e^{-r^2/\sigma^2} \tag{21}$$

In a spherical geometry, the "effective shell" of the particle—the region contributing most significantly to the interaction with the vacuum due to the volumetric factor $4\pi r^2$—is located at the characteristic radius $r \approx \sigma$.

At this boundary ($r = \sigma$), the source density decays to exactly $1/e$ of its peak value:

$$\frac{\rho(\sigma)}{\rho(0)} = e^{-1} \tag{22}$$

For a standing wave (soliton) to maintain energetic coherence, the vacuum coupling g must be strong enough to sustain the interaction not just at the dense core, but at this effective boundary. If we define the *Vacuum Impedance Z* as requiring a unitary interaction strength at the effective radius, the coupling constant g must compensate for the geometric decay of the source.

Thus, we postulate a renormalization condition:

$$g_{eff} \cdot \frac{\rho(\sigma)}{\rho(0)} \sim 1 \implies g \cdot e^{-1} \sim \text{const} \implies g \propto e \tag{23}$$

This suggests that the factor $k = e$ acts as a geometric gain coefficient, boosting the coupling strength exactly enough to overcome the natural exponential decay of the source envelope at its coherence scale. This ensures that the feedback loop receives a signal robust enough to maintain phase-locking, providing a theoretical basis for the stability observed in the numerical simulations.

4.4 Stability and Adiabatic Separation

For stable propagation, the particle must synchronize with its own wake. We define a feedback mechanism where the local field intensity modulates the internal frequency $\Omega(t)$ and its phase $\theta(t)$. The system evolves according to the coupled equations:

$$\dot{\Omega}(t) = -\alpha \bar{D}(t) \sin(\theta(t)) \tag{24a}$$

$$\dot{\theta}(t) = \Omega(t) \tag{24b}$$

$$\bar{D}(t) = \int_0^\infty D(r,t)\rho_\sigma(r)\, 4\pi r^2 dr \tag{24c}$$

where $\bar{D}(t)$ is the effective field potential sampled by the Gaussian envelope of the source (Eq. 1). Note that in the numerical implementation (Sec. 4.2), this feedback integral is evaluated along the radial ray using the volumetrically normalized source density, effectively projecting the 3D interaction onto the 1D simulation domain. The coupling constant α (with dimensions $[L^{-3}]$ in our units) determines the strength of the feedback sensitivity.

This mechanism forces the particle to phase-lock with the pilot wave. As shown in the simulation results, following a transient relaxation period, the system converges to a stable plateau where $\dot{\Omega} \to 0$, ensuring the adiabatic stability required for quantization.

While $\hbar_{eff}$ scales dynamically with the vacuum state, the internal pulse rate is significantly faster than the rate of change of the global vacuum density D. This separation of timescales ensures that local measurements perceive $\hbar_{eff}$ as a fixed constant in the present epoch [4, 10].

5 Numerical Verification

To validate the energetic stability criteria, we implemented a Finite-Difference Time-Domain (FDTD) simulation of the scalar field dynamics in the particle's rest frame. Specifically, we modeled the 'Breather' mode—the stationary pulsing soliton which forms the structural basis of the Walker. While the kinematic 'walking' behavior requires symmetry breaking in higher dimensions, the establishing of the frequency-coupling relation ($g \propto \sqrt{\Omega}$) in the radial rest frame is the prerequisite for the emergence of stable inertia.

To capture the physical energy scaling of a 3D particle while maintaining computational efficiency, we implemented a spherically symmetric (1D radial) simulation. Crucially, the source term ρ_σ applies the full 3D volumetric normalization ($\rho \propto \sigma^{-3}$) rather than a 1D linear normalization. This ensures that the coupling dynamics reflect the energy density of a 3D soliton, even while the wave propagation is modeled along a single radial ray.

The system was initialized using an exact Green's function solution to the static Klein-Gordon equation to establish the correct initial field topology. Absorbing "sponge" boundaries were applied to the grid edges to simulate an unbounded vacuum manifold.

Crucially, throughout the parameter sweep described in Sec. 4.2, we enforced the full geometric coupling law derived in Eq. 19:

$$g(\Omega, \sigma) = e \cdot \sigma^{5/2}\sqrt{\Omega} \tag{25}$$

where e is Euler's number. By varying both the particle size σ and the field mass μ, we ensured that the resulting stability is a robust geometric invariant rather than an artifact of specific units. The internal frequency $\Omega(t)$ was allowed to evolve dynamically according to the phase-locking feedback loop (Eq. 24), and the system autonomously converged to the stable states presented in Figure 3.

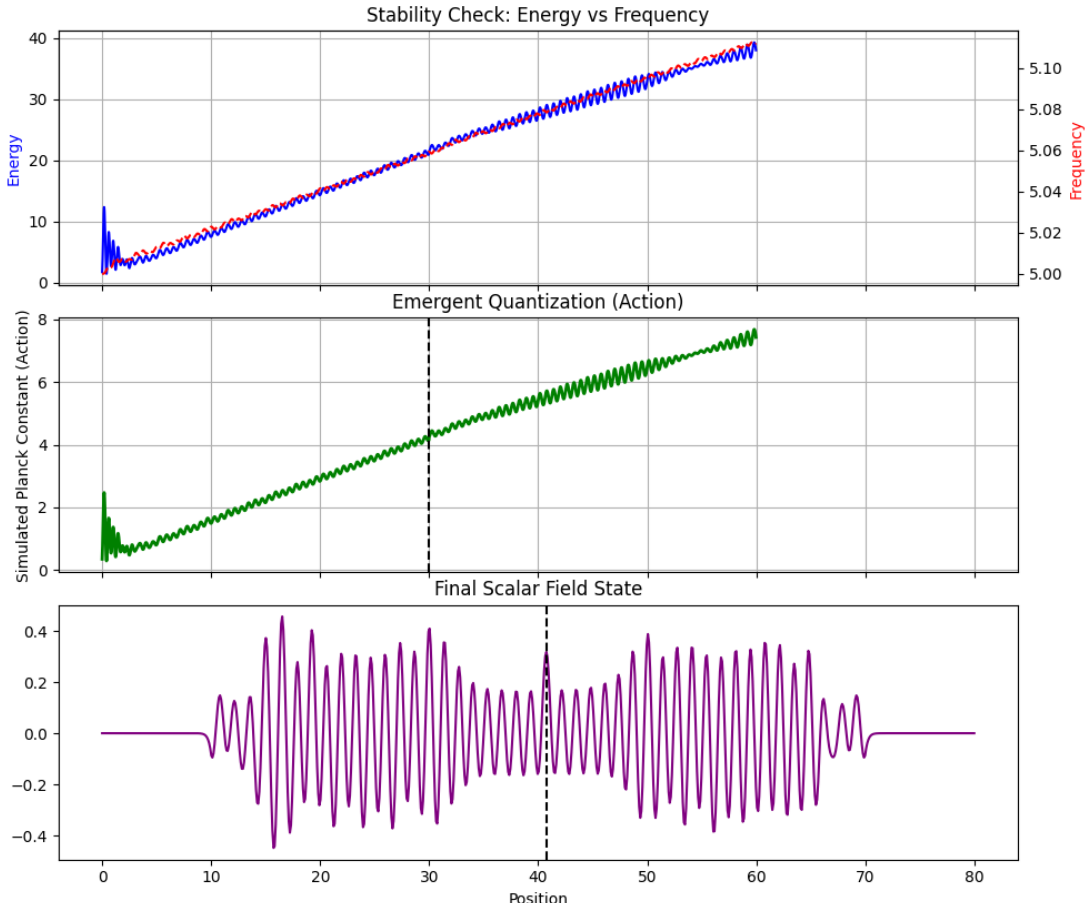

Figure 3: **Dynamics of Action and Vacuum State. Top:** Under acceleration, the particle interacts with varying vacuum potential, causing the internal frequency to adjust. **Middle:** The simulated action ($\hbar_{eff} = E/\Omega$) is observed to evolve. This is consistent with the model's core premise: while the *geometric scaling law* (governed by e) is fundamental and invariant, the *effective Planck constant* is a dynamic variable determined by the local vacuum density D. **Bottom:** Snapshot of the scalar field packet.

As observed in the initial phase (Fig. 3, top), the system undergoes a brief relaxation period as the dynamic coupling stabilizes. Following this transient, the soliton naturally seeks an adiabatic equilibrium. Crucially, this stability is maintained only when the coupling strength is tuned to the natural exponential scaling ($g \propto e$), suggesting that the vacuum impedance is governed by natural logarithmic growth. As shown in the middle plot, the action ($\hbar_{eff}$) is not a fixed universal constant but scales with the integrated history of the vacuum interaction.

6 Analytical Derivation of Inertia as Hydrodynamic Added Mass

In this framework, Newton's Second Law is not axiomatic but emerges from the interaction between the source and its pilot wave [8]. The self-force on an accelerating walker is derived by integrating the field gradient over its physical extent, allowing the particle to "sample" the pressure landscape it creates:

$$F_{self} = -g(\Omega)\cos(\theta(t)) \int d^3x \rho_\sigma(x - x_p)\nabla D(x,t) \tag{26}$$

For a soliton maintaining a quasi-rigid structure, any change in particle velocity $\dot{x}_p$ requires a corresponding update to the global field configuration. According to D'Alembert's principle, the reaction force from the vacuum fluid opposes this change [4]. This reaction is proportional to the time rate of change of the field momentum P_{field}:

$$F_{self} \approx -\frac{dP_{field}}{dt} = -m_{added}\ddot{x}_p \tag{27}$$

where $\ddot{x}_p$ denotes the particle's acceleration vector. The hydrodynamic added mass coefficient m_{added} is physically determined by the total field energy derived in Eq. 11 ($m_{added} \approx E_{field}/c^2 \propto g^2/\sigma$). We now apply the equation of motion for a core with zero intrinsic mass ($m_0 = 0$), balancing the external force F_{ext} against the vacuum reaction:

$$m_0\ddot{x}_p = F_{ext} + F_{self} \implies 0 = F_{ext} - m_{added}\ddot{x}_p \tag{28}$$

Rearranging terms recovers the familiar Newtonian form:

$$F_{ext} = m_{added}\ddot{x}_p \tag{29}$$

Thus, inertia is identified physically not as an intrinsic property, but as the drag of the vacuum fluid displaced by the accelerating soliton, directly analogous to the hydrodynamic memory drag observed in walking droplets [6, 8]. This constitutes a hydrodynamic realization of Mach's Principle: the local inertia of a body is determined entirely by its coupling to the global vacuum manifold [2].

7 Recovery of Relativistic Dynamics from Hydrodynamic Principles

The association of effective mass with the momentum flux of a wave packet is a foundational result in classical wave mechanics. As established historically by Brillouin and Starr [3], any localized wave packet transporting energy E possesses an effective momentum mass given by $m = E/c^2$.In this section, we demonstrate that the Relativistic Walker naturally recovers this behavior. We show that the hydrodynamic momentum of the scalar field strictly mimics the relativistic momentum relation ($P = \gamma m v$), ensuring that the system is Lorentz-covariant without requiring relativity as an a priori postulate. To derive the mass-energy equivalence explicitly, we now restore physical dimensions (where c is finite). The energy of the rest-frame soliton is defined by the Hamiltonian integral of the scalar energy-momentum tensor T_{00}:

$$E_{total} = \int \left[\frac{1}{2c^2} \left(\frac{\partial D}{\partial t} \right)^2 + \frac{1}{2}(\nabla D)^2 + \frac{1}{2}\mu^2 D^2 \right] d^3x = \hbar_{eff}\Omega \tag{30}$$

7.1 Mass-Energy Equivalence via Momentum Flux

To establish mechanical equivalence, we analyze the momentum carried by the moving wave packet. For a localized scalar envelope transporting energy at group velocity v_g, the momentum density $\mathcal{P}_i = T_{0i}/c$ is related to the energy density $\mathcal{E} = T_{00}$ under the wave-packet approximation:

$$\vec{P}_{field} = \int \frac{\mathcal{E}}{c^2} \vec{v}_g d^3x = \frac{E_{total}}{c^2} \vec{v}_g \tag{31}$$

We now *identify* the hydrodynamic momentum of the wave packet as the physical momentum observed in mechanics ($\vec{p}_{mech} \equiv \vec{P}_{field}$). Comparing this to the standard definition $\vec{p}_{mech} = m_{phys}\vec{v}_g$, we determine the proportionality constant:

$$m_{phys}\vec{v}_g = \frac{E_{total}}{c^2}\vec{v}_g \implies E_{total} = m_{phys}c^2 \tag{32}$$

Substituting the frequency relation derived in Eq. 19 yields the unified identity:

$$m_{phys}c^2 = \hbar_{eff}\Omega \tag{33}$$

This confirms that $E = mc^2$ is not an independent postulate, but the necessary dispersion relation for a standing wave packet possessing inertia.

8 Discussion: Toward a Unified Hydrodynamic Field

The rigorous derivation of inertia and quantization from scalar field dynamics suggests that the Relativistic Walker framework may extend beyond single-particle mechanics. We briefly outline how this hydrodynamic approach offers a unified narrative for fundamental interactions and quantum non-locality, recovering the phenomenology of the standard model from vacuum geometry.

8.1 Unification of Forces via Phase Dynamics

In this framework, the four fundamental forces are interpreted not as distinct fields, but as emergent behaviors of the scalar substrate D in different asymptotic limits:

- **Electromagnetism (Phase Interference):** Interactions between charged particles arise from the long-range interference of pilot waves. Constructive interference ($\Delta\theta \approx 0$) creates attractive potential wells, while destructive interference generates repulsive pressure barriers, reproducing Coulomb phenomenology via phase modulation.

- **Weak Interaction (Frequency Instability):** Decay processes are interpreted as phase-locking failures. The weak force acts as the restoring force $\dot{\Omega} \propto \bar{D}\sin(\theta)$ attempting to stabilize the particle's internal clock against vacuum fluctuations. A failure of this synchronization results in a "slip" to a lower, stable harmonic (decay).

- **Strong Interaction (Vortex Saturation):** At short ranges ($r < 1/\mu$), the field is dominated by the exponential Yukawa profile. This represents the hydrodynamic suction between vortex cores, providing the confinement force required for nuclear stability.

- **Gravity (Pressure Deficit):** Macroscopic bodies act as hydrodynamic sinks. The conservation of momentum induces a convergent flow ($v \propto r^{-1/2}$), creating a Bernoulli pressure deficit ($\Delta D \propto 1/r$). Since the wave speed scales with vacuum stiffness ($c \propto \sqrt{D}$), this gradient creates the effective refractive index responsible for gravitational attraction [7].

8.2 Hydrodynamic Entanglement

Finally, the model offers a deterministic resolution to Bell's inequalities. Entangled pairs are viewed as solitons riding a single, non-separable vacuum mode. While the "hidden variable" (the fluid configuration) is global and context-dependent, the local marginal probabilities remain statistical (50/50). This allows the system to violate Bell's inequality via hydrodynamic contextuality while strictly preserving the No-Signaling theorem.

8.3 Cosmological Implications: A Path Toward Emergent Time and Asymmetry

The hydrodynamic formulation of the vacuum, governed by the scalar field D and the geometric coupling g, offers a qualitative path toward resolving two specific cosmological anomalies without introducing additional fields.

1. The Divergence of Thermodynamic Age: In this framework, the internal clock of matter is not absolute but dynamically coupled to the local energy density via the relation $E \propto \Omega$ (derived in Eq. 33). In the early universe, where the scalar field density and interaction rates were extremized, the internal frequency Ω would ostensibly diverge relative to the geometric expansion rate. This suggests a bifurcation between the *geometric age* (measured by global expansion) and the *thermodynamic age* (measured by the integral of internal cycles). Matter present at this epoch would undergo vast thermodynamic evolution within a brief geometric interval, potentially offering a mechanism for the early structural maturity of galaxies observed by JWST, derived solely from the variable clock rates inherent to the model.

2. Vacuum Chirality and Antimatter Selection: The treatment of the vacuum as a physical superfluid suggests that the ground state may possess a global chiral order parameter (macroscopic angular momentum). In such a scenario, the symmetry between matter and antimatter acts as a symmetry between modes propagating with or against the vacuum flow. Rather than requiring distinct annihilation mechanisms, a chiral vacuum background would naturally stabilize the mode aligned with the global flow (matter) while suppressing the counter-rotating mode (antimatter) as energetically unfavorable. This frames the baryon asymmetry not as a violation of fundamental laws, but as a hydrodynamic selection principle inherent to a chiral vacuum substrate.

9 Conclusion

The Relativistic Walker model provides a rigorous derivation of the fundamental laws of motion and quantization from a single hydrodynamic source term. Rather than assuming quantum mechanics and relativity as separate axioms, we have shown that they are mathematically inevitable consequences of a scalar field interaction. The core contributions of this framework are the derivation of three emergent identities:

1. **The Geometric Stability Law:** We demonstrated that a pulsing soliton is stable only if its coupling strength scales with the square root of its frequency, governed by Euler's number:

$$g(\Omega) \approx e \cdot \sigma^{2.5}\sqrt{\Omega}$$

2. **Emergent Quantization:** This stability constraint forces the total energy to scale linearly with frequency, defining the effective action as a dynamic variable of the vacuum state rather than a fixed universal constant:

$$\hbar_{eff} \equiv \frac{E_{total}}{\Omega} \sim \mathcal{O}(L^4)$$

3. **The Origin of Inertia and Mass:** By identifying the reaction force of the vacuum fluid as hydrodynamic added mass ($F = m_{added}a$), we recovered the mass-energy equivalence as the dispersion relation for a standing wave packet:

$$E = m_{phys}c^2$$

By establishing the mechanical origin of $\hbar$, m, and c, this framework sets the stage for a unified treatment of gravitational and cosmological phenomena, suggesting that the "constants" of nature are in fact structural properties of the vacuum geometry.

Acknowledgments

Declaration of Generative AI and AI-Assisted Technologies in the Writing Process

During the preparation of this work, the author used Large Language Models (Gemini 3 Pro, ChatGPT-5.2) in order to improve language clarity, format LaTeX equations, and verify the dimensional consistency of derivations. After using these tools, the author reviewed and edited the content as needed and takes full responsibility for the content of the publication.

References

[1] P. A. M. Dirac, "Classical theory of radiating electrons," *Proc. R. Soc. Lond. A*, 167, 148, 1938.

[2] D. W. Sciama, "On the origin of inertia," *Mon. Not. R. Astron. Soc.* **113**, 34 (1953).

[3] L. Brillouin, *Wave Propagation and Group Velocity*, Academic Press, New York, 1960.

[4] L. D. Landau and E. M. Lifshitz, *Mechanics*, 3rd Ed., Butterworth-Heinemann, 1976.

[5] G. E. Volovik, *The Universe in a Helium Droplet*, Oxford University Press, 2003.

[6] Y. Couder and E. Fort, "Single-particle diffraction and interference at a macroscopic scale," *Phys. Rev. Lett.*, 97, 154101, 2006.

[7] C. Barceló, S. Liberati, and M. Visser, "Analogue Gravity," *Living Rev. Relativ.*, 14, 3, 2011.

[8] J. W. M. Bush, "Pilot-wave hydrodynamics," *Annu. Rev. Fluid Mech.*, 47, 269, 2015.

[9] J. W. M. Bush, "Hydrodynamic quantum field theory: the onset of particle motion," *Philos. Trans. Royal Soc. A*, 378, 20190534, 2020.

[10] E. Di Valentino et al., "In the realm of the Hubble tension—a review of constraints," *Class. Quant. Grav.* **38**, 153001 (2021).